Pharm Res (2012) 29:1582–1594
DOI 10.1007/s11095-012-0669-9

RESEARCH PAPER

PEG-Stabilized Micellar System with Positively Charged Polyester Core for Fast pH-Responsive Drug Release

Hua-Fen Wang • Hui-Zhen Jia • Si-Xue Cheng • Jun Feng • Xian-Zheng Zhang • Ren-Xi Zhuo

Received: 28 July 2011 / Accepted: 3 January 2012 / Published online: 21 January 2012

ABSTRACT

Purpose To design functional drug carriers for fast pH-responsive drug release.

Methods Functional diblock terpolymers of monomethoxy poly (ethylene glycol)-block- copoly(6,14-dimethyl-1,3,9,11-tetraoxa-6,14-diaza-cyclohexadecane-2,10-dione-*co*-ε-caprolactone) [*m*PEG-*b*-poly(ADMC-*co*-CL)] were fabricated via biosynthetic pathway. The self-assembled nanosphere and drug-loaded micelles of the copolymers were further prepared by dialysis method. The pH-tunable morphology variation and drug release pattern were observed at different pH.

Results A collection of three PEGylated terpolymers with varied compositions in poly(ADMC-*co*-CL) block was designed with high cell-biocompatibility. The copolymers could readily self-assemble into nanoscale micelles (~ 100 nm) in aqueous medium and exhibit high stability over 80-h incubation in different mediums including deionized water, neutral NaCl solution, and heparin sodium solution. Due to the protonation-deprotonation of tertiary amine groups in ADMC units, acid-induced structural deformation of micelles was disclosed in terms of the variation in CAC value and hydrodynamic size at different pH. Drug loading efficiency was comparable to that of reported PEG-polyester micelles with specifically designed structures purposed for drug-loading improvement. Remarkably accelerated drug release triggered by acidity was distinctly detected for ibuprofen-loaded *m*PEG-*b*-poly(ADMC-*co*-CL) micelle system, suggesting a fast pH-responsive characteristic.

Conclusion Functional PEG-stabilized micellar carriers with positively charged polyester core were successfully developed for fast pH-responsive drug release.

Electronic supplementary material The online version of this article (doi:10.1007/s11095-012-0669-9) contains supplementary material, which is available to authorized users.

H.-F. Wang • H.-Z. Jia • S.-X. Cheng • J. Feng (✉) • X.-Z. Zhang • R.-X. Zhuo
Key Laboratory of Biomedical Polymers (The Ministry of Education)
Department of Chemistry, Wuhan University
Wuhan 430072, China
e-mail: bmp_lab@hotmail.com

KEY WORDS cationic polycarbonate · diblock terpolymer · *m*PEG-*b*-poly(ADMC-*co*-CL) · pH-tunable drug release · polymeric micelles

INTRODUCTION

Since the past decade, polymeric micelles have been receiving more and more attention in use as drug delivery carriers. Those micelles are usually constructed from amphiphilic block copolymers composed of hydrophobic and hydrophilic polymeric segments. The block copolymers would readily undergo phase-separation and self-assemble into core-shell nanostructure in aqueous medium. The hydrophobic polymeric core could act as micro-container for efficient loading of poorly water-soluble drugs, leading to sustained drug release and minimized drug-associated side effects (1,2).

So far, poly(ethylene glycol) (PEG) is the mostly investigated polymer used as the hydrophilic building block for micelle formulation and its *in vivo* application has been approved by FDA (3-5). The flexible PEG outer shell would protect drug-loaded micelles from the reticulo-endothelial system (RES) ingestion (so-called stealth effect), and enhance the targeting efficiency against tumor tissues by the enhanced permeability and retention effect (EPR effect) (6,7). Given the consideration of biodegradability and biocompatibility, the micelles constructed from PEG-polyester copolymers, such as poly(ethylene glycol)-polylactide (PEG-PLA), poly(ethylene glycol)-poly(ε-caprolactone) (PEG-PCL), poly(ethylene glycol)-poly(lactide-*co*-glicolide) (PEG-PLGA), etc. appear to hold a leading position in the fundamental and applied field of pharmaceutical sciences (3-5,8). Nevertheless, some issues still remain in the applications of those micelles including unsatisfactory drug-loading efficiency, low polymer-drug compatibility,

lack of specific targeting and difficult control on the drug release rate according to specified requirements (5).

Currently, the attempts to address those issues are usually directed at the specifically designed incorporation of functional components or groups into the core-forming polyester chains (9-12). Such strategy permits appropriate regulation on the physicochemical properties of micellar carriers including hydrophilicity, degradation rate, permeability, micellar structural stability and so on. In particular, the functional groups located within the micelle core provide a new avenue for efficient drug loading via covalent, hydrogen-bonding or electrostatic interactions with drug molecules besides hydrophobic driving force (13-16).

A future aim for drug delivery will be the development of "smart" carriers. Those carriers could undergo conformational and structural change, phase transition in an environment-responsive manner and in turn dynamically tailor the release behavior of embedded drugs (17-20). We hypothesize that in addition to the possible property improvements, the integration of amine-containing cationic moieties into PEG-polyester may also provide the self-assembled micelles with structural metastability, depending on the susceptibility of micellar charge density, hydrophilicity, chain conformation and aggregated state in response to local stimulus (such as varied pH and ionic strength) (20-22). This feature is favorable for the formulation of smart drug delivery system used in electrolyte-enriched physiological environment. Furthermore, the buffer capability of amino groups is expected to, at least partly, counterbalance the side effects including the aseptic inflammation and drug deactivation caused by the acid intermediates after polyester degradation (23-25). Also, the positive charge of micelles may benefit the cellular uptake by negatively charged cell membrane through nonreceptor-mediated endocytosis, leading to effective intracellular therapy. Nevertheless, previous studies have disclosed that on the *in vivo* level, the nanoparticles with high cationic charges would suffer from rapid clearance by the RES upon the non-specific association with blood components, serum proteins and vessel endothelia (26). In this regard, it appears to be appropriate to construct a micellar nanostructure having a positive charged core coated by PEG shell with specific "stealth" function in terms of the *in vivo* application for the controlled drug release, especially for small molecule drugs.

Despite many expected advantages, the researches concerning the cationic modification towards the PEG-coated polyester core are rather limited and still challengeable at present (22). That is mainly due to tedious amine-associated protection-deprotection procedure, and the difficulties to yield compositionally and architecturally consistent products owing to the serious aminolysis of polyesters involved in preparation and storage process (27,28). Further, the biodegradability of introduced components should be paid significant attention from safety consideration.

In this paper, a facile strategy was established to introduce biodegradable cationic moieties into the core domain of PEG-polyester micelles. Recently, we reported a water-soluble and biodegradable cationic polycarbonate of poly(6,14-dimethyl-1,3,9,11-tetraoxa-6,14-diaza- cyclohexadecane-2,10-dione), (polyADMC), functionalized with tertiary amine groups in the backbone (29). Herein, ADMC units were further utilized as integral components to construct PEG-stabilized micelles with positively charged polyester core. As a representative example, functionalized *m*PEG-*b*-poly(ADMC-*co*-CL)s were prepared via one-pot enzymatic ROP (Scheme 1). Ibuprofen is an important non-steroidal anti-inflammatory drug used for the relief of rheumatoid arthritis and osteoarthritis, and has a neuroprotective effect against the risk of developing Parkinson's disease (30). Herein, it is employed to explore the potentials of nanosized *m*PEG-*b*-poly(ADMC-*co*-CL) micelles used for the delivery of hydrophobic drugs. Note that ibuprofen itself contains a -COOH group, it can also approximately serve as a model to preliminarily investigate the influence of electrostatic interactions between anionic drugs/proteins and the positively charged core within *m*PEG-*b*-poly(ADMC-*co*-CL) micelles with regard to drug-loading efficiency and drug release rate.

MATERIALS AND METHODS

Materials

Monomethoxy poly(ethylene glycol) (*m*PEG, M_n=2,000 g/mol) was purchased from Sigma and dried in *vacuo* at 100°C for 24 h before use. $(ADMC)_2$ was prepared according to our previous work (29). ε-CL purchased from Sigma was distilled under reduced pressure over calcium hydride (CaH_2) before use. Novozym-435 (lipase B from *Candida antarctica*) was purchased from Sigma and was vacuum dried over P_2O_5 (40 Pa, 25°C, 4 h) before use. Molecular sieve-4 Å was dehydrated at 400°C for 6 h. Toluene (Shanghai Chemical Reagent Company) was distilled under Na-K alloys before use. All other solvents

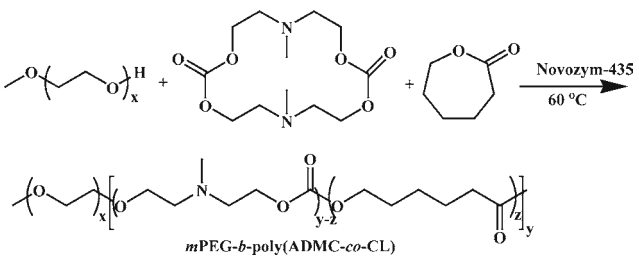

Scheme 1 Lipase-catalyzed synthesis of *m*PEG-*b*-poly(ADMC-*co*-CL) diblock terpolymer.

and reagents were used as received without further purification.

Preparation of *m*PEG-*b*-poly(ADMC-*co*-CL) Copolymers

Diblock terpolymer *m*PEG-*b*-poly(ADMC-*co*-CL) was synthesized via one-pot copolymerization of $(ADMC)_2$ and ε-caprolactone (ε-CL) in the presence of *m*PEG. Novozym-435 lipase was herein used as the catalyst for the copolymerization. The typical preparation of *m*PEG-*b*-poly(ADMC-*co*-CL)-a was described as follow: 50 mg dried *m*PEG, 100 mg $(ADMC)_2$ (0.34 mmol) and 100 mg ε-CL (0.88 mmol) were charged into a tube equipped with a magnetic stirring bar. 0.4 mL of dried toluene (v/w ratio = 2, toluene *versus* the total mass of comonomers) and some molecular sieves were introduced into the tube. After stirring for 2 h at room temperature, 20 mg of Novozym-435 (10% w/w relative to the comonomers) was added. The tube was immersed in the oil bath thermostated at 60°C. After 24 h reaction, the reaction mixture was cooled and diluted with 5 mL dichloromethane. The insoluble Novozym-435 was then filtrated away. After concentration with a rotary evaporator at reduced pressure, the residual solution was dropped into a great amount of ether to isolate the precipitated polymers. This precipitation process was repeated for three times thus obtaining the purified polymer. The polymerization conditions of *m*PEG-*b*-poly(ADMC-*co*-CL)-a, b, c are included in Table 1. For all the copolymers, the total amounts of two monomers in feed were fixed at about 200 mg irrespective of the monomer ratio. The yields of all samples were above 80%.

Polymer Characterization

Nuclear magnetic resonance (NMR) spectra of the samples were recorded on a Mercury VX-300 spectrometer at 300 Hz in $CDCl_3$ at the concentrations of ~4% (w/v). Copolymer $M_{n(NMR)}$ was determined by comparing the integral areas (A_{mPEG}) of the signal at δ 3.6 ppm (four methylene protons of *m*PEG) to that of ADMC unit at δ 2.74 ppm (four methylene protons adjacent to the N atom, (-CH_2CH_2N(CH_3)CH_2CH_2OCO-)) (A_{ADMC}) and that of CL unit at δ 1.62 ppm (four methylene protons, -$OCH_2CH_2CH_2CH_2CH_2CO$-) (A_{CL}) as follow:

$$Mn_{(NMR)} = 2000 + 2000 \times 145A_{ADMC}/44A_{mPEG} + 2000 \times 114A_{CL}/44A_{mPEG}$$

Fourier transformed infrared (FTIR) spectra were recorded on Perkin Elmer-2 spectrophotometer. The molecular weight distributions (M_w/M_n) of the products were measured by gel-permeation chromatography (GPC) calibrated with polystyrene standards. It was carried out on a Waters HPLC system equipped with a Model 2690D separation module, a Module 2410 differential refractive index detector and a Shodex K803 column. THF was used as eluent at a flow-rate of 1.0 ml/min. The sample concentration and injection volume was 0.3% (wt/v) and 20 μL, respectively. The weight- and number-average molecular weight ($M_{w(GPC)}$ and $M_{n(GPC)}$) were calculated from a calibration curve using a series of polystyrene standards with molecular weight ranging from 1,300 to 30,000.

The thermal property of the terpolymers was measured by a differential scanning calorimetry (DSC) (Perkin-Elmer Pyris-1). The copolymers were subjected to DSC measurements in an identical manner with a heating rate of 10°C/min and a cooling rate of 5°C/min in the range of −60°C to 100°C under the steady flow of nitrogen.

Micelle Formation

The micelles of *m*PEG-*b*-poly(ADMC-*co*-CL) terpolymers were prepared by a membrane-dialysis method. Briefly, *m*PEG-*b*-poly(ADMC-*co*-CL) copolymers were dissolved in THF at an initial concentration of 200 mg/L, and then subjected to dialysis against 2 L of deionized water for

Table 1 Reaction Conditions and Properties of *m*PEG-*b*-poly(ADMC-*co*-CL) Diblock Terpolymers [IV]

Sample [I]	Feed ratio (wt%)			Composition (wt%) [II]			M_n [II]	M_n [III]	M_w/M_n [III]
	PEG [IV]	$(ADMC)_2$	CL	PEG	ADMC	CL	–	–	–
1	20	40	40	18.8	38.4	42.8	10600	9100	1.73
2	20	20	60	18.6	18.9	62.5	10700	12400	1.77
3	20	13	67	20.4	11.4	68.2	9900	15100	1.72

[I] Sample 1, 2 and 3 were labeled as *m*PEG-*b*-poly(ADMC-*co*-CL)-a, b and c, respectively

[II] determined by ^{1}H NMR analyses

[III] determined by GPC

[IV] M_n of *m*PEG used was 2,000 g/mol and the M_w/M_n was 1.56

24 h using a dialysis tube (molecular weight cut-off: 3,500 g/mol). The deionized water was replaced every 4 h to remove THF.

TEM Measurement

Transmission electron microscope (TEM) was measured by JEM-100CX II at an acceleration voltage of 100 keV. In brief, a drop of micelle suspension, obtained just as above, was placed on a copper grid with formvar film and stained by a 0.2% (w/v) solution of phosphotungstic acid before measurement.

Fluorescence Measurement and Determination of CAC

Fluorescence spectra were recorded on a LS55 luminescence spectrometer (Perkin-Elmer). Pyrene was used as a hydrophobic fluorescent probe. Aliquots of pyrene solutions (1×10^{-3} M in acetone, 6 μL) were added to containers, and the acetone was allowed to evaporate at 60°C. Ten-milliliter aqueous dispersion with different copolymer concentrations was then added to the containers. Note that all the aqueous samples contained pyrene at the same concentration of 6×10^{-7} M. The solutions were kept at room temperature for 24 h to reach the solubilization equilibrium of pyrene in the aqueous phase. Emission was carried at 393 nm, and excitation spectra were recorded ranging from 300 to 360 nm. Excitation and emission bandwidths were 10 and 5 nm, respectively. From the pyrene excitation spectra, the change of the intensity ratio (I_{337}/I_{334}; higher ratios mean a less polar environment) was plotted against the logarithm of the copolymer concentrations. The critical aggregation concentration (CAC) was determined based on the crossover point at low polymer concentration on this plot (31,32). For the CAC determination at pH 5.0, the pH was adjusted by adding certain amount of concentrated HCl under a microprocessor pH meter.

Micelle Size and Micelle Stability

The mean particle size and size distribution of self-assembled micelles in aqueous medium were determined by means of dynamic light scattering (DLS) technique with a Nano-ZS ZEN3600 instrument. The samples were diluted to a concentration of 60 mg/L with distilled water and passed through a 0.45 μm pore size filter before measurement. To investigate the micelle stability in deionized water or 10% (w/w) heparin sodium (150 units/mg) solution, the variation of micelle diameter was monitored by DLS measurement at the predetermined time interval without filtration treatment. The salt effect on the micellar size was investigated with different NaCl concentration up to 1.2 mol/L at pH=3.7 and 7.0, respectively.

Drug Loading and *In Vitro* Drug Release

The experiments were carried out according to the references (4,33). *m*PEG-*b*-poly(ADMC-*co*-CL) copolymer (10 mg) and 4 mg of ibuprofen were dissolved in the mixed solvent containing 10 mL of THF and 2 ml of DMF. The solutions were put into a dialysis tube (molecular weight cut-off: 3,500 g/mol, Shanghai Chemical Reagent Co.) and then subjected to dialysis against 1 L of deionized water for 24 h. The deionized water was replaced every 4 h to remove the solvents and the unloaded drugs.

After drug loading, the dialysis tube was directly immersed into 400 mL of PBS (I=0.1 M) at pH=7.4 and 6.0 at 37.4°C for *in vitro* release test, respectively. Aliquots of 3 mL were withdrawn from the outer solution periodically. The volume of solution was remained constantly by adding 3 mL of PBS after each sampling. The amount of ibuprofen in PBS released from micelles was determined on the basis of the UV absorbance intensity at 264 nm (34), using a standard calibration curve experimentally obtained. The total mass of loaded drug contained the cumulative mass of drug released and the drug unreleased which still remained in the micelles. To determine the amount of unreleased drug, the micelle solution after drug release was lyophilized and dissolved in 10 mL of DMSO and the value was obtained by UV absorbance at 272 nm (35). We define the drug release efficiency (DRE), entrapment efficiency (EE) and drug loading efficiency (DLE) as follows:

DRE =(total mass of released drug at the determined time/mass of drug loaded in micelles)×100%

EE =(mass of drug loaded in micelles/mass of drug fed initially)×100%

DLE =(mass of drug loaded in micelles/mass of drug-loaded micelles)×100%

Cell Culture

COS7 cells and HeLa cells were incubated in Dulbecco's Modified Eagle's Medium (DMEM) containing 10% fetal bovine serum (FBS) and 1% antibiotics (penicillin-streptomycin, 10,000 U/mL) at 37°C in a humidified atmosphere containing 5% CO_2.

Cytotoxicity Assay

The cytotoxicity of *m*PEG-*b*-poly(ADMC-*co*-CL) was evaluated by MTT assay (36). For each well in a 96-well plate, the number of COS7 cells and HeLa cells in each well were 6×10^3, respectively. After incubation for 24 h in an incubator (37°C, 5% CO_2), the cells were then incubated for 48 h in the culture media containing the copolymers at various concentrations up to 110 mg/L. After that, the medium was replaced

with 200 μL of fresh medium and 20 μL MTT (3-(4,5-dimethylthiazol-2-yl)-2,5-diphenyl tetrazolium bromide) (5 mg/ml) solutions. After incubation for 4 h, the medium was removed and 200 μL DMSO was added to dissolve the formazan crystals. The optical density (OD) was measured spectrophotometrically in an ELSA plate reader (model 550, Bio-Rad, USA) at a wavelength of 570 nm. We defined the cell viability as: cell viability (%)=($OD_{570(samples)}/OD_{570(control)}$)×100%, where $OD_{570(samples)}$ represents the absorbance of the solution containing *m*PEG-*b*-poly(ADMC-*co*-CL) in the well and $OD_{570(control)}$ corresponds to the absorbance of the solution without *m*PEG-*b*-poly(ADMC-*co*-CL) addition.

RESULTS AND DISCUSSION

Synthesis and Structure of Diblock *m*PEG-*b*-poly (ADMC-*co*-CL) Terpolymers

The diblock *m*PEG-*b*-poly(ADMC-*co*-CL) terpolymers were prepared via one-pot copolymerization of $(ADMC)_2$ and ε-CL in the presence of *m*PEG (M_n=2,000 g/mol) (Scheme 1). In the ROP, the *m*PEG end-capped with one hydroxyl group served as the macroinitiator. Biosynthetic pathway like metal-free enzymatic polymerization has recently attracted great attention as a new approach for biomaterial synthesis (4,37,38). This straightforward method was utilized for the syntheses of *m*PEG-*b*-poly(ADMC-*co*-CL) copolymers. Given the high catalytic activity and the tolerance against functional groups, Novozym-435 lipase was herein used as the catalyst for the copolymerization (37,38). By adjusting the charge ratio of *m*PEG/ε-CL/$(ADMC)_2$ in feed, three copolymer products were eventually obtained and named as *m*PEG-*b*-poly(ADMC-*co*-CL)-a, *m*PEG-*b*-poly(ADMC-*co*-CL)-b and *m*PEG-*b*-poly(ADMC-*co*-CL)-c, respectively (Table 1).

The chemical structures of *m*PEG-*b*-poly(ADMC-*co*-CL) terpolymers were well-characterized by means of ^{1}H NMR and GPC analyses. ^{1}H NMR spectra of *m*PEG-*b*-poly (ADMC-*co*-CL) copolymers in $CDCl_3$ (Fig. 1) show the presence of characteristic resonances of *m*PEG-*b*-poly (ADMC-*co*-CL)s. The signal centered at δ 3.6 ppm with strong intensity is attributed to the -CH_2-CH_2-O- proton of *m*PEG segment. The characteristic resonance at δ 2.74 (-O-CH_2CH_2N(CH_3)CH_2CH_2OCO-) from ADMC units, and that at δ 2.30 ppm (-OC$H_2$$CH_2$$CH_2$$CH_2CH_2$CO-) belonging to CL units were distinctly detectable. The complex signals in the region of 4.0~4.3 disclose the random structure of poly(ADMC-*co*-CL) block. As shown in the expanded spectrum (Fig. 1), in addition to the resonances corresponding to ADMC-ADMC and CL-CL sequences, new-emerging signals at δ 4.12 ppm should be assignable to ADMC-CL (CL-ADMC) sequences.

The polymerization process of *m*PEG-*b*-poly(ADMC-*co*-CL)-a was monitored by GPC profiles (Fig. 2). In the elution curve of the mixture prior to polymerization (0 h curve), the

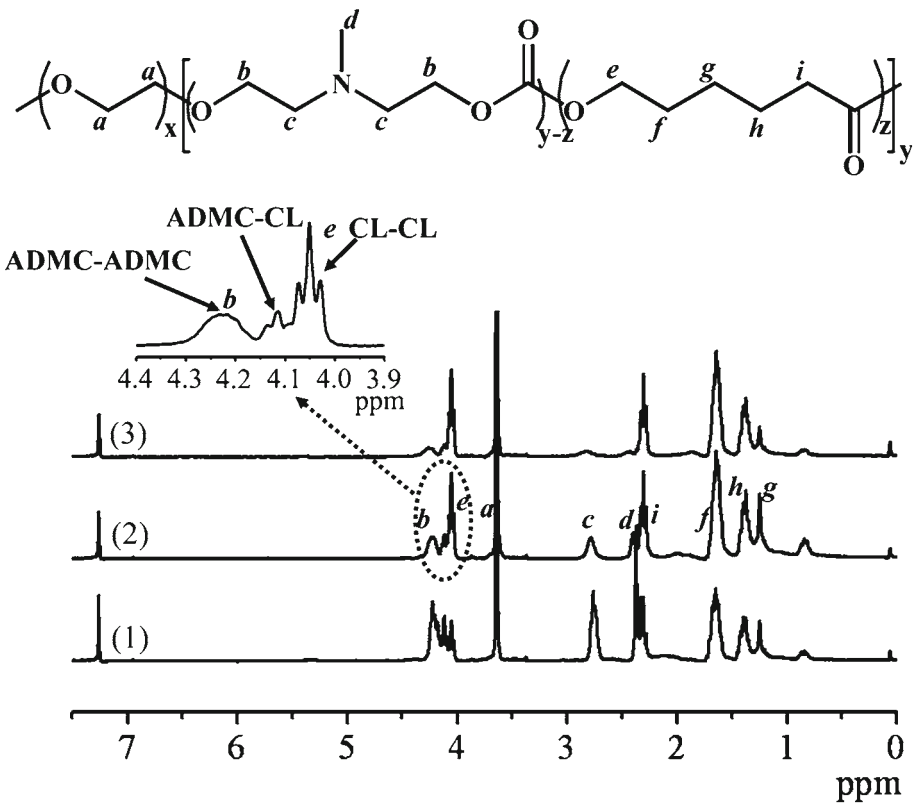

Fig. 1 ^{1}H NMR spectra of terpolymers including *m*PEG-*b*-poly(ADMC-*co*-CL)-a (**1**), *m*PEG-*b*-poly(ADMC-*co*-CL)-b (**2**), and *m*PEG-*b*-poly(ADMC-*co*-CL)-c (**3**).

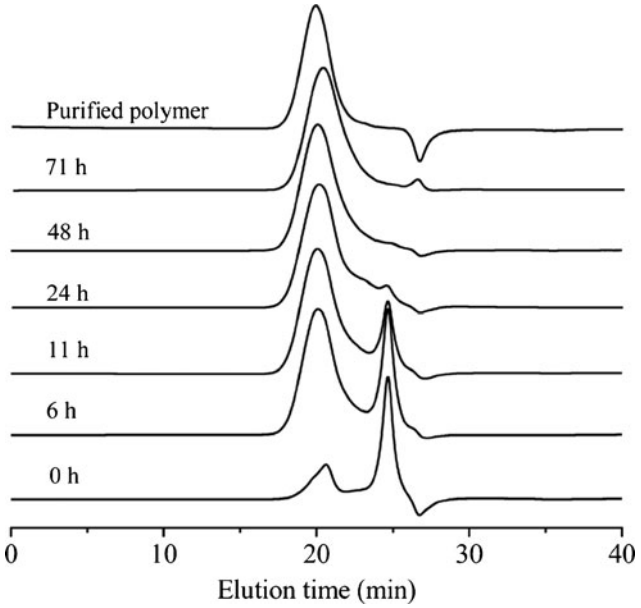

Fig. 2 Polymerization process of *m*PEG-*b*-poly(ADMC-*co*-CL)-a monitored by GPC profiles.

peak at short retention time was assignable to the *m*PEG and the other corresponded to the comonomers. As reaction proceeded, the intensity of the comonomer signal showed a gradual decrease accompanied by a simultaneous increase in that of polymer. Besides, an increase in the polymer molecular weight was clearly shown in the GPC chromatogram. At about 24 h, the comonomer signal almost disappeared but just the polymer signal was detectable, suggesting the complete consumption of the monomers. Note that the molecular weight of the products after 71 h reaction was slightly lower than that of 48 h product, indicative of degradation occurrence when further prolonging the reaction. Only a unimodal symmetric peak with a moderate distribution existed in the GPC curve of the purified copolymer, suggesting that the homopolymerization may be ignored in the present study.

The polymerization conditions and results are summarized in Table 1. The resultant data suggest that the copolymer structure can be finely tailored in a controllable manner. For the obtained copolymers, the copolymer composition and $M_{n(NMR)}$ determined by NMR analyses agreed well with those theoretically calculated from the feed ratios. As a result, the respective M_ns of hydrophobic poly(ADMC-*co*-CL) blocks in three terpolymers are very close, thus allowing the exclusive investigation on the relationship between copolymer composition and properties. The deviation between $M_{n(NMR)}$ and $M_{n(GPC)}$ obtained by GPC is possibly related to the specific amphiphilic feature of *m*PEG-*b*-poly(ADMC-*co*-CL) as well as the marked difference between the copolymers and the GPC calibration standards of polystyrene.

Taken together, all those experimental results strongly demonstrate the successful syntheses of diblock *m*PEG-*b*-poly(ADMC-*co*-CL) terpolymers. Our convenient strategy provides precise control on the polymer composition while avoiding the protection-deprotection procedure. This advantage sounds appealing since one knows, the polymer properties greatly rely on the polymer composition. More attractively, it may be potentially developed as a universal strategy for the cationic modification of most of the existing PEG-*b*-polyester copolymers usually prepared from ROP of parent lactones and lactides with the PEG initiation.

Thermal Properties of *m*PEG-*b*-poly(ADMC-*co*-CL) Copolymers

The thermal characteristics of diblock terpolymers were investigated by DSC analyses. Both *m*PEG (M_n=2,000 g/mol) and PCL are semicrystalline polymers and their melting transition temperatures (T_m) are 59 and 60°C, respectively. In comparison, polyADMC has been demonstrated as an amorphous polymer (29). Evident differences were observed between the DSC diagrams of *m*PEG-*b*-poly(ADMC-*co*-CL)-a, b, and c (Fig. 3). In the DSC curves of the samples, the presence of the double endothermic peaks clearly indicates the melting transition of *m*PEG block and PCL segment. When the ADMC content increases, the T_m corresponding to the peak at high temperature is almost unchanged while the other one presents a significant shift towards lower temperature. Obviously, the T_m peak at high temperature should be attributed to *m*PEG block and the other one belongs to PCL segment. An explanation to this phenomenon would be assigned to the inhibited packing amongst PCL chains as a result of the disturbances by ADMC incorporation. Indeed, as increasing ADMC content, the average chain length of PCL segment

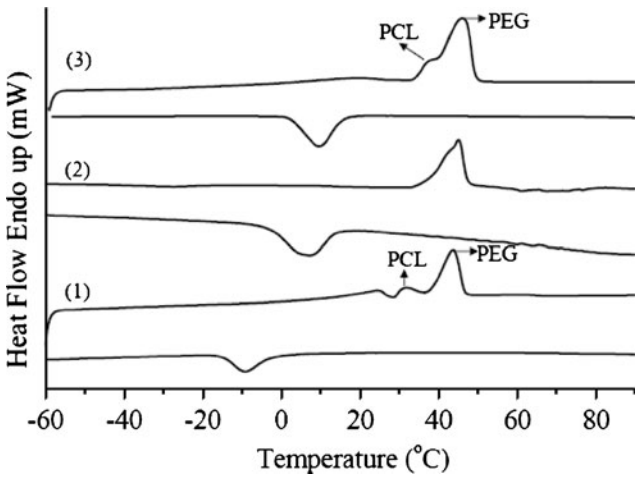

Fig. 3 DSC curves of the terpolymers (*m*PEG-*b*-poly(ADMC-*co*-CL)-a (**1**), *m*PEG-*b*-poly(ADMC-*co*-CL)- b (**2**), and *m*PEG-*b*-poly(ADMC-*co*-CL)-c (**3**).

becomes shorter and the crystallizing capacity would decline (39). In contrast, due to the unique block structure, such influence seems not significant on the crystallization of PEG block. This conclusion was reconfirmed by the fact that only one exothermic peak appears in the cooling curve, which corresponds to the crystallizing transition of *m*PEG block, while that of PCL is lost (4). Moreover, for the given PEG length (M_n=2,000 g/mol), the crystallizing transition of PEG occurs at lower temperature in the case of higher ADMC content. It suggests that the presence of ADMC units would retard the crystallization of *m*PEG blocks to some extent (4,40). The DSC analyses reinforce the block structure of *m*PEG-*b*-poly(ADMC-*co*-CL)s. The thermal properties of micelle-forming copolymers may exert some effects on the micellar delivery system. In general, stronger crystallization in the core domain would lead to better micellar stability and relatively difficult diffusion of embedded drugs out from micelles (1,4).

Formation of *m*PEG-*b*-poly(ADMC-*co*-CL) Polymeric Micelles

Fluorescence spectra of pyrene provide some useful information about its local environments. The formation of the micelles from *m*PEG-*b*-poly(ADMC-*co*-CL) copolymers in aqueous medium was verified by a pyrene probe technique. When polymeric micelles form, pyrene is preferentially distributed in the hydrophobic micelle core rather than in the hydrophilic outer shell, thus the local environment around pyrene is changed from polar to non-polar. Along with such change, a red-shift from 334 to 337 nm took place in the excitation spectra upon the aggregation of *m*PEG-*b*-poly(ADMC-*co*-CL) copolymers in aqueous medium. Hence the intensity ratios of I_{337}/I_{334} were constructed as a function of *m*PEG-*b*-poly(ADMC-*co*-CL) concentrations to determine critical aggregation concentration (CAC).

A negligible change of I_{337}/I_{334} ratios was detected at the low concentration range, but at a certain concentration the ratio exhibited a substantial increase, indicating the onset of micelle formation. The CAC was thus determined from the crossover point at the low concentration range. As shown in Fig. 4a–c, the CAC value for *m*PEG-*b*-poly(ADMC-*co*-CL)-a, *m*PEG-*b*-poly(ADMC-*co*-CL)-b and *m*PEG-*b*-poly(ADMC-*co*-CL)-c was 13.49, 7.08, 4.27 mg/L, respectively. It is evident that the CAC values of *m*PEG-*b*-poly(ADMC-*co*-CL)s are largely dependent on the composition of poly(ADMC-*co*-CL) block. With the decreasing ADMC content, CAC value shows a decreasing tendency and the copolymers seem to form micelles more readily. Generally speaking, stronger hydrophobicity of the core-forming polymers would facilitate the micelle formation driven by the force to minimize the interfacial free energy. Therefore, the decline in CAC value of *m*PEG-*b*-poly(ADMC-*co*-CL) series should be mainly due to the stronger hydrophobic interactions within the "core" domain in the case of higher CL contents.

The morphology and size distribution of polymer micelles were investigated by transmission electron microscopy (TEM) and dynamic light scattering (DLS). The micelles were prepared by dialysis method. During the process, the solution changed from transparency to translucency, partly proving the formation of micelles. The representative TEM image and DLS profile of *m*PEG-*b*-poly(ADMC-*co*-CL)-a are shown in

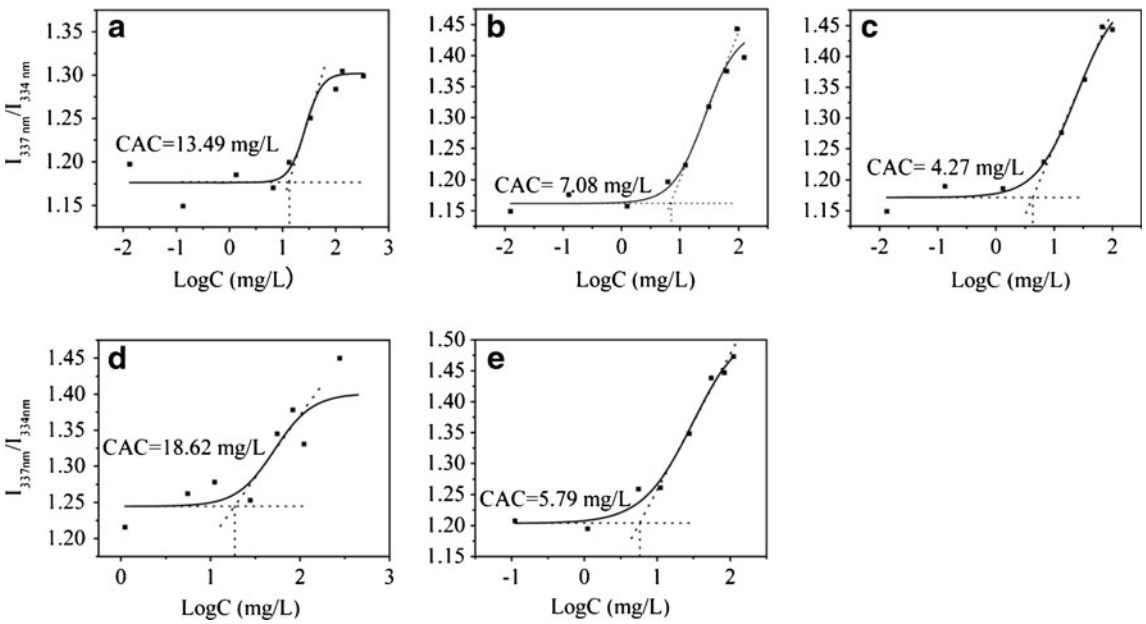

Fig. 4 I_{337}/I_{334} plotted as a function of *m*PEG-*b*-poly(ADMC-*co*-CL) copolymer concentration. (**a**) *m*PEG-*b*-poly(ADMC-*co*-CL)-a at pH=7, (**b**) *m*PEG-*b*-poly(ADMC-*co*-CL)-b at pH=7, (**c**) *m*PEG-*b*-poly(ADMC-*co*-CL)-c at pH=7, (**d**) *m*PEG-*b*-poly(ADMC-*co*-CL)-b at pH=5, (**e**) *m*PEG-*b*-poly(ADMC-*co*-CL)-c at pH=5.

Fig. 5. From the TEM image in Fig. 5a, the core-shell structure could be distinctly observed. The self-assembled micelles were well dispersed as individual nanoparticles with an average diameter at about 40 nm. There is insignificant difference amongst three copolymers with respect to the nanoparticle size observed by TEM. The micelles are regularly spherical without secondary aggregation observed between individual micelles. In comparison, the hydrodynamic diameter of *m*PEG-*b*-poly(ADMC-*co*-CL)-a micelle determined by DLS (Fig. 5b) was around 98±7 nm. The deviation between the micelle sizes measured by DLS and TEM should be attributed to the fact that the former is the hydrodynamic diameter of micelle in water, whereas the latter reveals the morphology size of the micelle in dry state. Similar differences in size as a result of different measuring techniques were also reported elsewhere (4). The average hydrodynamic diameters of *m*PEG-*b*-poly(ADMC-*co*-CL)-b and *m*PEG-*b*-poly(ADMC-*co*-CL)-c micelle were 100±5 nm and 115±5 nm, respectively (Fig. S1). In addition to CAC analyses, TEM and DLS results reinforce the self-assembly of *m*PEG-*b*-poly(ADMC-*co*-CL) terpolymers into nanosized micelles in aqueous medium.

It has been reported that endocytosis by many types of mammalian cells was limited to the particles less than 150 nm in diameter (41). Furthermore, tissues of the reticulo-endothelial system, liver, spleen, and bone marrow have a sinusoidal endothelial structure permitting relatively free passage of materials within a size distribution of 100 nm. The above results indicate that *m*PEG-*b*-poly(ADMC-*co*-CL) micelles can be developed as potentially efficient drug carriers for drug release purpose.

Stability of *m*PEG-*b*-poly(ADMC-co-CL) Polymeric Micelles

The diameter of the micelles was monitored by DLS as a function of incubation time up to 80 h to evaluate the stability of the micelles in deionized water. The micellar average size varies little during the observation period (Fig. 6a) especially for mPEG-b-poly(ADMC-co-CL)-a and mPEG-b-poly(ADMC-co-CL)-b, indicating the reasonable stability of micellar structures. In addition to the steric hindrance caused by freely extending PEG chains, the charge repulsion originating from cationic ADMCs may also contribute to the stability to some extent thus preventing the secondary aggregation of micelles.

To assess the serum-conditioned stability of the micelles, the DLS measurement was further challenged in the serum-imitated condition with the coexistence of heparin. Here, highly negatively charged heparin was used on behalf of negatively charged serum components. No obvious change in the micelle size is observed for mPEG-b-poly(ADMC-co-CL)-b and c micelles upon contact with heparin sodium during an 80-h period (Fig. 6b). Relatively, that of mPEG-b-poly(ADMC-co-CL)-a with the highest ADMC content presents a very slight increment after 60 h, which can be explained by the electrostatic attraction between the positively charged ADMC units and the negatively charged heparin.

Overall, the mean size of mPEG-b-poly(ADMC-co-CL) micelles varies little during the observation period. Such stability is advantageous for *m*PEG-*b*-poly(ADMC-*co*-CL)s in use as drug carriers, since it may lead to long circulating time *in vivo* and thus allow for desirable drug bioavailability and more efficient accumulation in tumor tissues at specified condition such as with the aid of passive and/or active target (6,7).

pH Effect on Morphology of *m*PEG-*b*-poly(ADMC-*co*-CL) Micelles

It is expected that polyADMC would share many features of polyelectrolyte due to the presence of a number of ionizable tertiary amine groups along polymer chains (29). PolyADMC would exhibit different hydration capacity with the specific environment variation. Unlike traditional amphiphilic block copolymers where the hydrophobic segments lack ionic or hydrophilic components, the presence of ADMC units would affect the thermodynamic stability of the micelles in response to external stimuli (pH or ionic strength). Those advantages in combination with the special PEG-associated functions may provide *m*PEG-*b*-poly(ADMC-*co*-CL) copolymers great

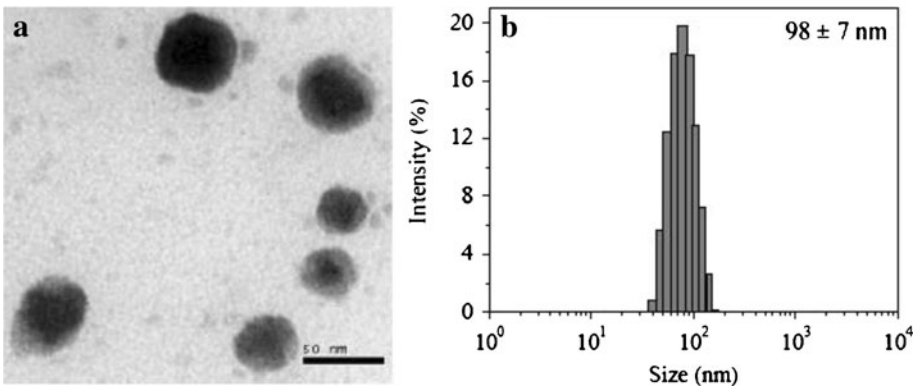

Fig. 5 TEM image (**a**) and size distribution (**b**) of the *m*PEG-*b*-poly(ADMC-*co*-CL)-a micelle prepared in deionized water.

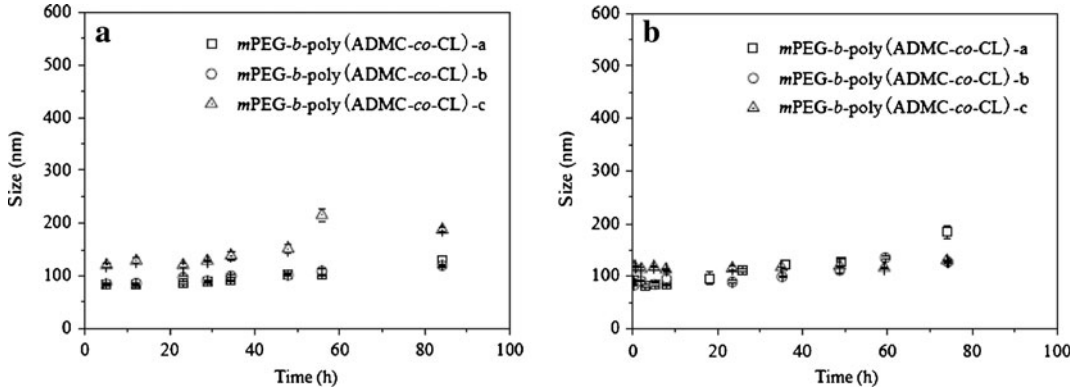

Fig. 6 Variation of *m*PEG-*b*-poly(ADMC-*co*-CL) micelle diameters determined by DLS as a function of incubation time. The experiment was conducted at 25°C with the polymer concentration at 60 mg/L in deionized water (**a**) and in 10% (w/w) heparin sodium solution (**b**).

potentials for use as smart soft materials. Herein, a preliminary study was conducted regarding the pH-sensitivity of *m*PEG-*b*-poly(ADMC-*co*-CL) micelles.

We examine the size variation of *m*PEG-*b*-poly(ADMC-*co*-CL)-a micelles by DLS when changing the solution pH. The micelles were firstly prepared at pH=7.34 and the solution pH were then adjusted by adding concentrated HCl or NaOH solution. As seen from Fig. 7, the size of *m*PEG-*b*-poly(ADMC-*co*-CL)-a micelles gradually increased and then remained almost unchanged when decreasing pH from 7.34 to 2.15. This finding can be explained in such a way as illustrated in Scheme 2. Once ADMC is protonated upon acidification, the enhanced hydrophilicity within the core domain would compromise the polymer association driven by the hydrophobic interaction. On the other hand, the ionization degree of ADMC units increases with the decreasing pH level, leading to strengthened electrostatic repulsion among the positively charged copolymer chains. Consequently, stronger repulsive interactions together with weaker hydrophobic associations make for much looser micellar structure and the volume

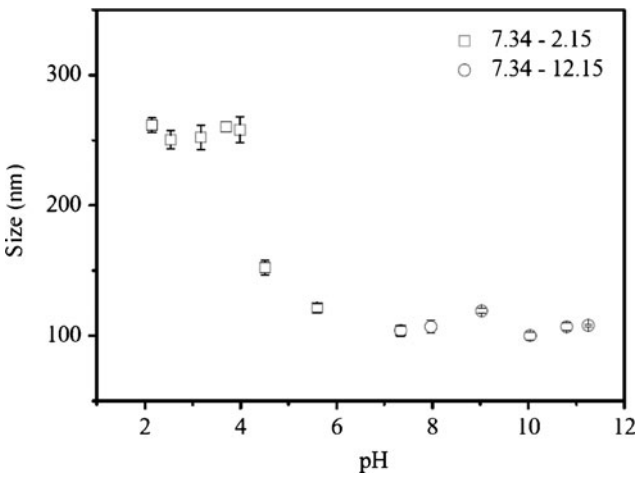

Fig. 7 Size variation of *m*PEG-*b*-poly(ADMC-*co*-CL)-a micelle as a function of pH value. The experiment was conducted at 25°C with the polymer concentration at 60 mg/L.

expansion of micelles. Nevertheless, when the ADMC units are completely protonated, further decrease in pH would exert little influence on such structural variation and the micelle size remains constant. Based on this hypothesis, it is thus not difficult to understand why nearly no change in the micellar size was detected when increasing pH from 7.34 to 11.5 (Fig. 7).

To acquire more information about such pH-sensitive behavior, the CAC of *m*PEG-*b*-poly(ADMC-*co*-CL)s was measured for comparison purpose at pH=7 and 5, respectively by fluorescence spectroscopy. The results shown in Fig. 4d, e indicate that, CAC values would become larger when the solution pH was increased from 7 to 5. Such increase in the CAC values implies that the micelles prepared at pH=7 may undergo structural destabilization more or less upon acidification (32). The method of fluorescence spectroscopy using pyrene as probe seems not applicable for the CAC determination at pH=5 with regard to *m*PEG-*b*-poly(ADMC-*co*-CL)-a having the highest ADMC content. It was possibly due to the strong hydrophilicity of poly(ADMC-co-CL)-a block in the acid condition. As far as the polarity of pyrene-located environment is concerned, perhaps there is no significant difference between the micellar core and the aqueous medium at the given condition. Though the CAC of *m*PEG-*b*-poly(ADMC-*co*-CL)-a cannot be provided, it is obvious that the increment of CAC upon acidification were presented more profoundly in the case of higher ADMC content in the copolymers.

Salt Effect on Morphology of *m*PEG-*b*-poly(ADMC-*co*-CL) Micelles

To investigate the salt effect on the morphology of *m*PEG-*b*-poly(ADMC-*co*-CL) micelles, the sizes variation of *m*PEG-*b*-poly(ADMC-*co*-CL) micelles with increasing NaCl concentration was monitored by DLS (Fig. 8). At pH=7.0, three *m*PEG-*b*-poly(ADMC-*co*-CL) polymers exhibited no or insignificant changes regarding micelle size irrespective of NaCl concentration, strongly reconfirming the structural stability of the micelles in neutral aqueous medium. Nevertheless, at pH=

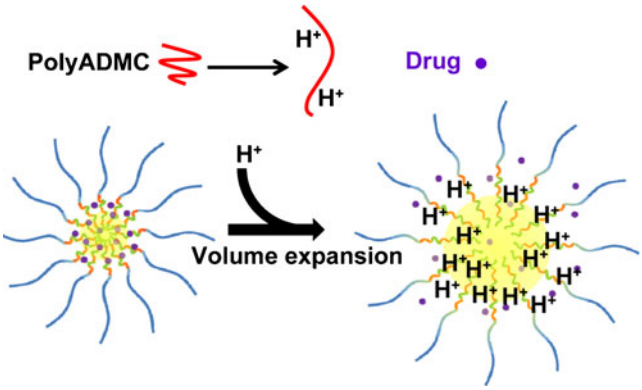

Scheme 2 Schematic illustration of the pH-sensitive variation of micellar morphology and drug release pattern.

3.7, the increased NaCl concentration above 0.7 mol/L lead to an apparently increment of *m*PEG-*b*-poly(ADMC-*co*-CL)-a micelle size. In comparison, such salt-sensitivity was presented insignificantly for *m*PEG-*b*-poly(ADMC-*co*-CL)-b and c with relatively lower ADMC contents. Evidently, the salt effect observed at acid medium should have strong association with the ionization of ADMC units. (42).

Drug Loading and Release

Ibuprofen is a non-steroidal anti-inflammatory drug used for the relief of rheumatoid arthritis and osteoarthritis (4,30,34). Nevertheless, its therapeutic use is relatively limited due to the frequent side effects and poor water-solubility. In this study, ibuprofen was used as the model drug to evaluate the potential of PEG-b-poly(ADMC-co-CL) micelles as delivery carriers for the hydrophobic drugs.

The entrapment efficiency (EE) was determined as 27.8%, 27.3% and 29.8% while the corresponding drug loading efficiency (DLE) of ibuprofen was 11.1%, 10.9% and 11.9% for PEG-b-poly(ADMC-co-CL)-a, b and c micelles, respectively. There is no significant difference amongst them although it is anticipated that higher ADMC content would lead to the enhanced drug-loading due to the electrostatic interaction between COOH-containing ibuprofen and ADMC units. For *m*PEG-*b*-poly(ADMC-*co*-CL) micelles, the randomly distributed ADMC units in hydrophobic block would inhibit the formation of a completely hydrophobic core. Therefore, the DLE is believed to be strongly affected by the simultaneously weakened hydrophobic interaction between drug and core-forming poly(ADMC-*co*-CL), leading to a compromised improvement on drug loading efficiency. As reported, the DLE of PEG-PCL micelle system for hydrophobic ibuprofen is less than 12% even when purposely introducing the hydrogen bond interaction, π−π stacking interaction and special structure such as miktoarm star structure to improve the drug-micelle compatibility (43,44). At this point, our micelle system is relatively satisfactory. In addition, the presence of ADMC units within micellar core may be likely an advantage for the encapsulation of negatively charged proteins and relatively hydrophilic anionic drugs owing to the electrostatic attraction.

After fabricating drug-loaded *m*PEG-*b*-poly(ADMC-*co*-CL) micelles, the *in vitro* release of ibuprofen was carried out in PBS (pH 7.4, ionic strength 0.1 M) at 37.4°C. The resultant data (Fig. 9) show a continuous ibuprofen release over 80 h from the micelles formulated with three *m*PEG-*b*-poly(ADMC-*co*-CL) terpolymers. No apparent difference is found amongst the release profiles of those drug-loaded micelles. This phenomenon can be explained as the consequence of two competitive drug-loading driving forces including hydrophobic and electrostatic interactions between polymer container and drug. The increased hydrophilicity and depressed crystallization of core-forming poly(ADMC-*co*-CL) due to ADMC introduction would allow for the drug diffuse out from micellar core into water phase with less

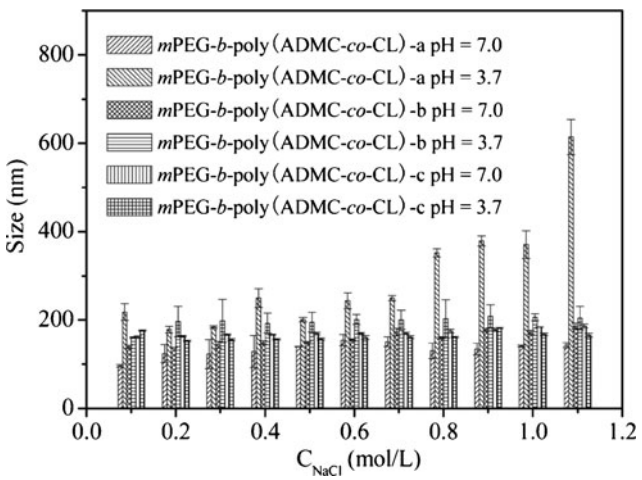

Fig. 8 Size variation of *m*PEG-*b*-poly(ADMC-*co*-CL) micelles at different NaCl concentration. The experiment was carried out at 25°C with a polymer concentration of 60 mg/L.

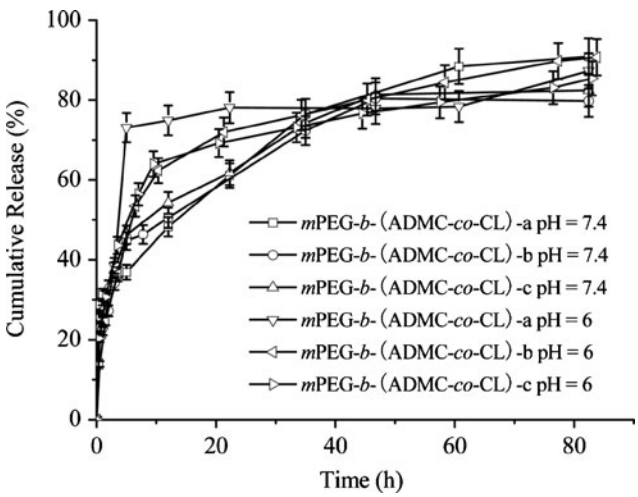

Fig. 9 Release profiles of Ibuprofen from terpolymer micelles.

difficulty. On the contrary, the more ADMC contents, the stronger electrostatic interaction between COOH-containing ibuprofen and ADMC units is, which retards the drug release (45).

Note that at lower pH=6.0, which is close to the pH of most solid tumors, the release of ibuprofen loaded in *m*PEG-*b*-poly(ADMC-*co*-CL) micelles was found to have a marked acceleration in the initial phase. After 5 h incubation, the released drug of *m*PEG-*b*-poly(ADMC-*co*-CL)-a micelle can reach as high as 73%, indicative of the high pH-dependence of the release behavior. Such fast pH-responsive drug release is seldom reported for polymeric micellar systems. Generally speaking, the ibuprofen release from matrix would be somewhat suppressed at acidic circumstance for the micelles prepared from common PEG-polyester copolymers. This is because that decreasing the pH would inhibit the ionization of COOH-containing ibuprofen, and ibuprofen molecules diffuse more slowly than its ionized counterparts. Based on the obtained results regarding the morphology and CAC variation at different pH, such acid-triggered rapid release of ibuprofen from *m*PEG-*b*-poly(ADMC-*co*-CL) micelles is believed to have association with the protonation of tertiary amine groups, which enhances the hydrophilicity of polymers and somewhat loosens the structure of *m*PEG-*b*-poly(ADMC-*co*-CL) micelles formed at pH=7.4 (Scheme 2). Another possible reason to be considered is that the acid environment would lessen the electrostatic interaction between polymer and drugs. Given those considerations, it is thus not difficult to explain the fact that the acid-induced release acceleration was presented more significantly for *m*PEG-*b*-poly(ADMC-*co*-CL)-a with the highest ADMC contents, suggesting the higher sensitivity to the decreased pH level.

The drug release acceleration in fast response to decreased pH levels, observed herein, sounds interesting from the viewpoint of the drug delivery specifically directed at the physiologically acidic environments including stomach and tumor as well as some cellular compartments such as endosome. For example, contrary to the normal blood pH of 7.4, the measured pH values of most solid tumors in patients range from pH 5.7 to 7.8. The appropriate nanosize (below 150 nm) of *m*PEG-*b*-poly(ADMC-*co*-CL) micelles would confer their accumulation in tumor tissue by a passive target mechanism. Such passive target might be strengthened since the acid-induced volume expansion of *m*PEG-*b*-poly(ADMC-*co*-CL) micelles would make the drug-loaded micelles more difficult to cross the membrane barrier and escape away from tumor sites. The locally acid microenvironment would also lead to fast release of loaded drugs within *m*PEG-*b*-poly(ADMC-*co*-CL) micelles, which can be approximately viewed as a "tumor-triggered targeting" (46). The establishment of the *m*PEG-*b*-poly(ADMC-*co*-CL) based drug delivery system, combining two targeting mechanisms mentioned above, would potentially provide a new way to deliver drugs effectively into tumor sites, and to reduce overall dosage and drug-associated side effects.

In Vitro Cytotoxicity Evaluation

The cytotoxicity of a vector for medical application is one of the critical factors determining whether it can be practically used in clinics. In this study, we performed a preliminary evaluation on the *in vitro* cytotoxicity of obtained copolymers by MTT assay. The cytotoxicity results of *m*PEG-*b*-poly(ADMC-*co*-CL)s in HeLa and COS7 cells are shown in Fig. 10. For both cells, the relative cell viability remains almost above 100% at the measured polymer concentration up to 110 mg/L. It reveals that *m*PEG-*b*-poly(ADMC-*co*-CL)s display very minimal cytotoxicity, indicative of the good cell-biocompatibility.

CONCLUSIONS

Functional PEG-stabilized micellar carriers with positively charged polyester core were successfully developed for fast pH-responsive drug release. A series of novel diblock terpolymers, *m*PEG-*b*-poly(ADMC-*co*-CL)s were synthesized via

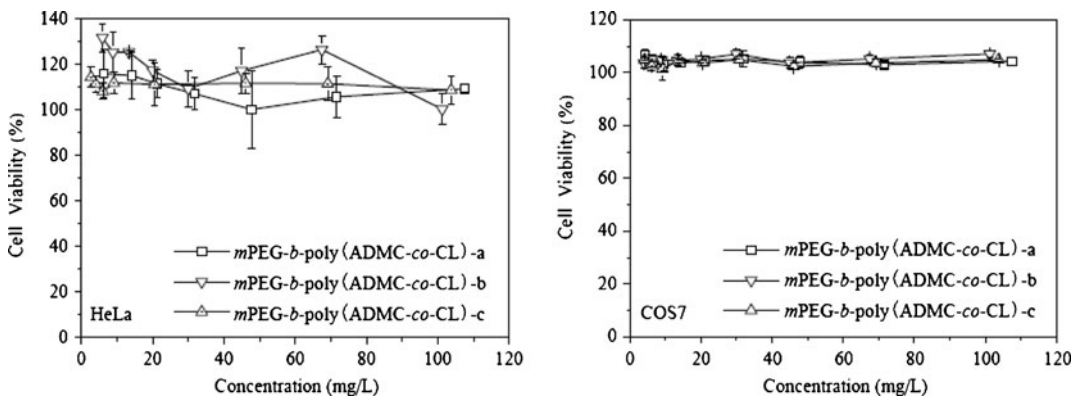

Fig. 10 *In vitro* cytotoxicity of *m*PEG-*b*-poly(ADMC-*co*-CL) polymeric micelles with different concentrations.

one-pot Novozym-435-catalyzed copolymerization of $(ADMC)_2$ and ε-CL in the presence of *m*PEG (M_n= 2,000 g/mol). The resultant data show that the copolymer M_n and composition agrees well with the charge ratio in feed, indicating the controllable feature of such method. Those obtained *m*PEG-*b*-poly(ADMC-*co*-CL)s can readily self-assemble into nanosized micelles in aqueous medium. The mean diameters of the micelles are around 100 nm determined by DLS and around 40 nm by TEM. The CAC values are dependent on the copolymer composition and the solution pH. The formed micelles exhibit high stability over 80 h with respect to the micellar size in different mediums including deionized water, neutral NaCl solution and heparin sodium solution, which is favorable to prolong the circulating time *in vivo* and thus allow for desirable drug bioavailability. In contrast, the micelle sizes are found to be sensitive to pH level and an apparently acid-induced volume expansion is observed for the micelles. The ibuprofen loading efficiency in the micelles is comparable to that of the reported PEG-polyester micelle systems with specifically designed structures purposed for drug-loading improvement. The sustained ibuprofen release from *m*PEG-*b*-poly (ADMC-*co*-CL) micelles is found to have a marked acceleration in the acidic condition, indicating a fast pH-responsive characteristic. The *in vitro* MTT assay shows that the obtained block terpolymers exhibit no apparent cytotoxicity in HeLa and COS7 cells. In summary, with further study, those novel diblock terpolymers and their micelles can be developed as potentially smart drug carriers in response to external pH stimulus at specific lesion sites.

ACKNOWLEDGMENTS & DISCLOSURES

This work was financially supported by the National Key Basic Research Program of China (2011CB606202 and 2009CB930301) and National Natural Science Foundation of China (Grant No. 20874075).

REFERENCES

1. Kataoka K, Harada A, Nagasaki Y. Block copolymer micelles for drug delivery: design, characterization and biological significance. Adv Drug Deliv Rev. 2001;47:113–31.
2. Torchilin VP. Micellar nanocarriers: pharmaceutical perspectives. Pharm Res. 2007;24:1–16.
3. Otsuka H, Nagasaki Y, Kataoka K. PEGylated nanoparticles for biological and pharmaceutical applications. Adv Drug Deliv Rev. 2003;55:403–19.
4. Feng J, Su W, Wang HF, Huang FW, Zhang XZ, Zhuo RX. Facile fabrication of diblock methoxy poly(ethylene glycol)-poly (tetramethylene carbonate) and its self-assembled micelles as drug carriers. ACS Appl Mater Interfaces. 2009;1:2729–37.
5. Schubert US, Knop K, Hoogenboom R, Fischer D. Poly(ethylene glycol) in drug delivery: pros and cons as well as potential alternatives. Angew Chem Int Edit. 2010;49:6288–308.
6. Iyer AK, Greish K, Seki T, Okazaki S, Fang J, Takeshita K, Maeda H. Polymeric micelles of zinc protoporphyrin for tumor targeted delivery based on EPR effect and singlet oxygen generation. J Drug Target. 2007;15:496–506.
7. Torchilin VP. Passive and active drug targeting: drug delivery to tumors as an example. Handb Exp Pharmacol. 2010;197:3–53.
8. Chan JM, Zhang LF, Yuet KP, Liao G, Rhee JW, Langer R, *et al.* PLGA-lecithin-PEG core-shell nanoparticles for controlled drug delivery. Biomaterials. 2009;30:1627–34.
9. Danquah M, Fujiwara T, Mahato RI. Self-assembling methoxypoly(ethylene glycol)-b-poly(carbonate-co-L-lactide) block copolymers for drug delivery. Biomaterials. 2010;31:2358–70.
10. Shi M, Ho K, Keating A, Shoichet MS. Doxorubicin-conjugated lmmuno-nanoparticles for intracellular anticancer drug delivery. Adv Funct Mater. 2009;19:1689–96.
11. Wang Y, Gao S, Ye WH, Yoon HS, Yang YY. Co-delivery of drugs and DNA from cationic core-shell nanoparticles self-assembled from a biodegradable copolymer. Nat Mater. 2006;5:791–6.
12. Yue J, Li XY, Mo GJ, Wang R, Huang YB, Jing XB. Modular functionalization of amphiphilic block copolymers via radical-mediated thiol-ene reaction. Macromolecules. 2010;43:9645–54.
13. Truong MT, Walker LM. Quantifying the importance of micellar microstructure and electrostatic interactions on the shear-induced structural transition of cylindrical micelles. Langmuir. 2002;18:2024–31.
14. Garbuzenko O, Zalipsky S, Qazen M, Barenholz Y. Electrostatics of PEGylated micelles and liposomes containing charged and neutral lipopolymers. Langmuir. 2005;21:2560–8.
15. Su W, Luo XH, Wang HF, Li L, Feng J, Zhang XZ, *et al.* Hyperbranched polycarbonate-based multimolecular micelle with enhanced stability and loading efficiency. Macromol Rapid Commun. 2011;32:390–6.
16. Kim SH, Tan JPK, Nederberg F, Fukushima K, Colson J, Yang CA, *et al.* Hydrogen bonding-enhanced micelle assemblies for drug delivery. Biomaterials. 2010;31:8063–71.
17. Ponta A, Bae Y. PEG-poly(amino acid) block copolymer micelles for tunable drug release. Pharm Res. 2010;27:2330–42.
18. Ganta S, Devalapally H, Shahiwala A, Amiji M. A review of stimuli-responsive nanocarriers for drug and gene delivery. J Control Release. 2008;126:187–204.
19. Lee ES, Oh KT, Kim D, You HH, Ahn YS. pH-sensitive properties of surface charge-switched multifunctional polymeric micelle. Int J Pharm. 2009;376:134–40.
20. Lee RS, Yang JM, Lin TF. Novel, biodegradable, functional poly (ester-carbonate)s by copolymerization of trans-4-hydroxy-L-proline with cyclic carbonate bearing a pendent carboxylic group. J Polym Sci Part A: Polym Chem. 2004;42:2303–12.
21. Lee ES, Shin HJ, Na K, Bae YH. Poly(L-histidine)-PEG block copolymer micelles and pH-induced destabilization. J Control Release. 2003;90:363–74.
22. Ni PH, Zhang WL, He JL, Liu Z, Zhu XL. Biocompatible and pH-Responsive triblock copolymer mPEG-b-PCL-b-PDMAEMA: synthesis, self-assembly, and application. J Polym Sci Part A: Polym Chem. 2010;48:1079–91.
23. Ceonzo K, Gaynor A, Shaffer L, Kojima K, Vacanti CA, Stahl GL. Polyglycolic acid-induced inflammation: role of hydrolysis and resulting complement activation. Tissue Eng. 2006;12:301–8.
24. Fu K, Pack DW, Klibanov AM, Langer R. Visual evidence of acidic environment within degrading poly (lactic-co-glycolic acid) (PLGA) microspheres. Pharm Res. 2000;17:100–6.

25. Walter E, Moelling K, Pavlovic J, Merkle HP. Microencapsulation of DNA using poly (L-lactide-co-glycolide): stability issues and release characteristics. J Control Release. 1999;61:361–74.
26. Peter J, Jaroslav PT, Merdan T, Waters J, Cheung K, Von GK, Culmsee C, Wagner E. Synthesis and characterization of chemically condensed oligoethylenimine containing beta-aminopropionamide linkages for siRNA delivery. Biomaterials. 2007;28:3731–40.
27. Wang CF, Lin YX, Jiang T, He F, Zhuo RX. Polyethylenimine-grafted polycarbonates as biodegradable polycations for gene delivery. Biomaterials. 2009;30:4824–32.
28. Knorr V, Russ V, Allmendinger L, Ogris M, Wagner E. Acetal linked oligoethylenimines for use as pH-sensitive gene carriers. Bioconjugate Chem. 2008;19:1625–34.
29. Wang HF, Su W, Zhang C, Luo XH, Feng J. Biocatalytic fabrication of fast-degradable, water-soluble polycarbonate functionalized with tertiary amine groups in backbone. Biomacromolecules. 2010;11:2550–7.
30. Gao X, Chen H, Schwarzschild MA, Ascherio A. Use of ibuprofen and risk of Parkinson disease. Neurology. 2011;76:863–9.
31. Ko J, Park K, Kim YS, Kim MS, Han JK, Kim K, *et al.* Tumoral acidic extracellular pH targeting of pH-responsive MPEG-poly (beta-amino ester) block copolymer micelles for cancer therapy. J Control Release. 2007;123:109–15.
32. Lee ES, Oh KT, Kim D, Youn YS, Bae YH. Tumor pH-responsive flower-like micelles of poly(L-lactic acid)-b-poly(ethylene glycol)-b-poly(L-histidine). J Control Release. 2007;123:19–26.
33. Wei H, Cheng C, Chang C, Chen WQ, Cheng SX, Zhang XZ, *et al.* Synthesis and applications of shell cross-linked thermoresponsive hybrid micelles based on poly(N-isopropylacrylamide-co-3-(trimethoxysilyl)propyl methacrylate)-b-poly(methyl methacrylate). Langmuir. 2008;24:4564–70.
34. Bidone J, Melo APP, Bazzo GC, Carmignan F, Soldi MS, Pires ATN, *et al.* Preparation and characterization of ibuprofen-loaded microspheres consisting of poly(3-hydroxybutyrate) and methoxy poly(ethylene glycol)-b-poly(D, L-lactide) blends or poly(3-hydroxybutyrate) and gelatin composites for controlled drug release. Mater Sci Eng C. 2009;29:588–93.
35. Chen JX, Wang HY, Li C, Han K, Zhang XZ, Zhuo RX. Construction of surfactant-like tetra-tail amphiphilic peptide with RGD ligand for encapsulation of porphyrin for photodynamic therapy. Biomaterials. 2011;32:1678–84.
36. Sun YX, Zeng X, Meng QF, Zhang XZ, Cheng SX, Zhuo R. X. The influence of RGD addition on the gene transfer characteristics of disulfide-containing polyethyleneimine/DNA complexes. Biomaterials. 2008;29:4356–65.
37. Veld MAJ, Palmans ARA, Meijer EW. Selective polymerization of functional monomers with Novozym 435. J Polym Sci Part A: Polym Chem. 2007;45:5968–78.
38. Deng F, Gross RA. Ring-opening bulk polymerization of epsilon-caprolactone and trimethylene carbonate catalyzed by lipase Novozym 435. Int J Biol Macromol. 1999;25:153–9.
39. Cristand B, Mirabella FM. Crystal thickness distributions from melting homopolymers or random copolymers. J Polym Sci Part B: Polym Phys. 1999;37:3131–40.
40. Zhang Z, Grijpma DW, Feijen J. Thermo-sensitive transition of monomethoxy poly(ethylene glycol)-block-poly(trimethylene carbonate) films to micellar-like nanoparticles. J Control Release. 2006;112:57–63.
41. Bishop NE. An update on non-clathrin-coated endocytosis. Rev Med Virol. 1997;7:199–209.
42. Beng HT, Kam CT, Yee CL, Chee B. Microstructure and rheology of stimuli-responsive nanocolloidal systems: effect of ionic strength. Langmuir. 2004;20:11380–6.
43. Suksiriworapong J, Sripha K, Kreuter J, Junyaprasert VB. Investigation of polymer and nanoparticle properties with nicotinic acid and p-aminobenzoic acid grafted on poly(ε-caprolactone)-poly(ethylene glycol)-poly(ε-caprolactone) via click chemistry. Bioconjugate Chem. 2011;22:582–94.
44. Gou PF, Zhu WP, Shen ZQ. Synthesis, self-assembly, and drug-loading capacity of well-defined cyclodextrin-centered drug-conjugated amphiphilic A14B7 miktoarm star copolymers based on poly(ε-caprolactone) and poly(ethylene glycol). Biomacromolecules. 2010;11:934–43.
45. Qu FY, Zhu GS, Lin HM, Sun JY, Zhang DL, Li SG, *et al.* Drug self-templated synthesis of ibuprofen/mesoporous silica for sustained release. Eur J Inorg Chem. 2006;19:3943–7.
46. Quan CY, Chen JX, Wang HY, Li C, Chang C, Zhang XZ, *et al.* Core-Shell nanosized assemblies mediated by the alpha-beta cyclodextrin dimer with a tumor-triggered targeting property. ACS Nano. 2010;4:4211–9.